Clinical Neurophysiology 121 (2010) 962–976

Contents lists available at ScienceDirect

Clinical Neurophysiology

journal homepage: www.elsevier.com/locate/clinph

Age trends in auditory oddball evoked potentials via component scoring and deconvolution

Cliff C. Kerr [a,b,*], Sacha J. van Albada [a,b], Christopher J. Rennie [a,b,c], Peter A. Robinson [a,b,d]

[a] School of Physics, University of Sydney, New South Wales 2006, Australia
[b] Brain Dynamics Centre, Westmead Millennium Institute, Sydney Medical School – Western, University of Sydney, Westmead Hospital, New South Wales 2145, Australia
[c] Department of Medical Physics, Westmead Hospital, Westmead, New South Wales 2145, Australia
[d] Sydney Medical School, University of Sydney, New South Wales 2006, Australia

ARTICLE INFO

Article history:
Accepted 18 November 2009
Available online 15 March 2010

Keywords:
Auditory oddball
Evoked potential
Component scoring
Deconvolution
Development
Aging
N1
N2
P2
P3

Objective: This study examines developmental and aging trends in auditory evoked potentials (AEPs) by applying two analysis methods to a large database of healthy subjects.
Methods: AEPs and reaction times were recorded from 1498 healthy subjects aged 6–86 years using an auditory oddball paradigm. AEPs were analyzed using a recently published deconvolution method and conventional component scoring. Age trends in the resultant data were determined using smooth median-based fits.
Results: Component latencies generally decreased during development and increased during aging. Deconvolution showed the emergence of a new feature during development, corresponding to improved differentiation between standard and target tones. The latency of this feature provides similar information as the target component latencies, while its amplitude provides a marker of cognitive development.
Conclusions: Age trends in component scores can be related to physiological changes in the brain. However, component scores show a high degree of redundancy, which limits their information content, and are often invalid when applied to young children. Deconvolution provides additional information on development not available through other methods.
Significance: This is the largest study of AEP age trends to date. It provides comprehensive statistics on conventional component scores and shows that deconvolution is a simple and informative alternative.

1. Introduction

Developmental and aging effects on auditory evoked potentials (AEPs) have been studied for over 40 years (Dustman and Beck, 1969). While certain findings have been widely observed, previous studies have also reported a number of conflicting results. Additionally, most previous studies have relied exclusively on component scoring as the method of AEP analysis. Our aim is to use a large dataset (1498 subjects) over a wide age range (6–86 years) to provide comprehensive statistics on developmental and aging changes in the AEP in terms of waveform morphologies, component scores, and a recently published deconvolution method (Kerr et al., 2009).

In this study, AEPs were evoked using the oddball paradigm, where an infrequent high-pitched ("target") tone, requiring a motor response, was interspersed with a frequent low-pitched ("standard") tone. The resultant AEPs to these two tone types are shown for several different ages in Fig. 1. Both types of responses undergo considerable morphological change during development (rows 1–3), as well as a more gradual quantitative change during aging (rows 3–4). In particular, the N1 component in targets and standards appears to be absent in most children under age 12 (Albrecht et al., 2000; Bishop et al., 2007). The adult morphologies for both standard and target AEPs emerge during adolescence, although changes in amplitudes and latencies of the components continue throughout life. In general, the waveforms of adults display much more differentiation between target and standard stimuli than those of children, almost certainly reflecting adults' improved capacity to categorize stimuli (Friedman and Simpson, 1994). It has also been reported that a deterioration in stimulus categorization ability exists in the elderly, but this does not produce qualitative changes in AEP morphology (Dujardin et al., 1993).

The most widely reported effect of age on oddball AEPs is an increase in P3 latency from young adulthood onwards, although estimates of the rate vary from 0.8 ms/year (Dujardin et al., 1993) to

* Corresponding author. Address: School of Physics, University of Sydney, New South Wales 2006, Australia. Tel.: +61 2 9036 7960; fax: +61 2 9351 7726.
E-mail address: ckerr@physics.usyd.edu.au (C.C. Kerr).

1388-2457/$36.00
doi:10.1016/j.clinph.2009.11.077

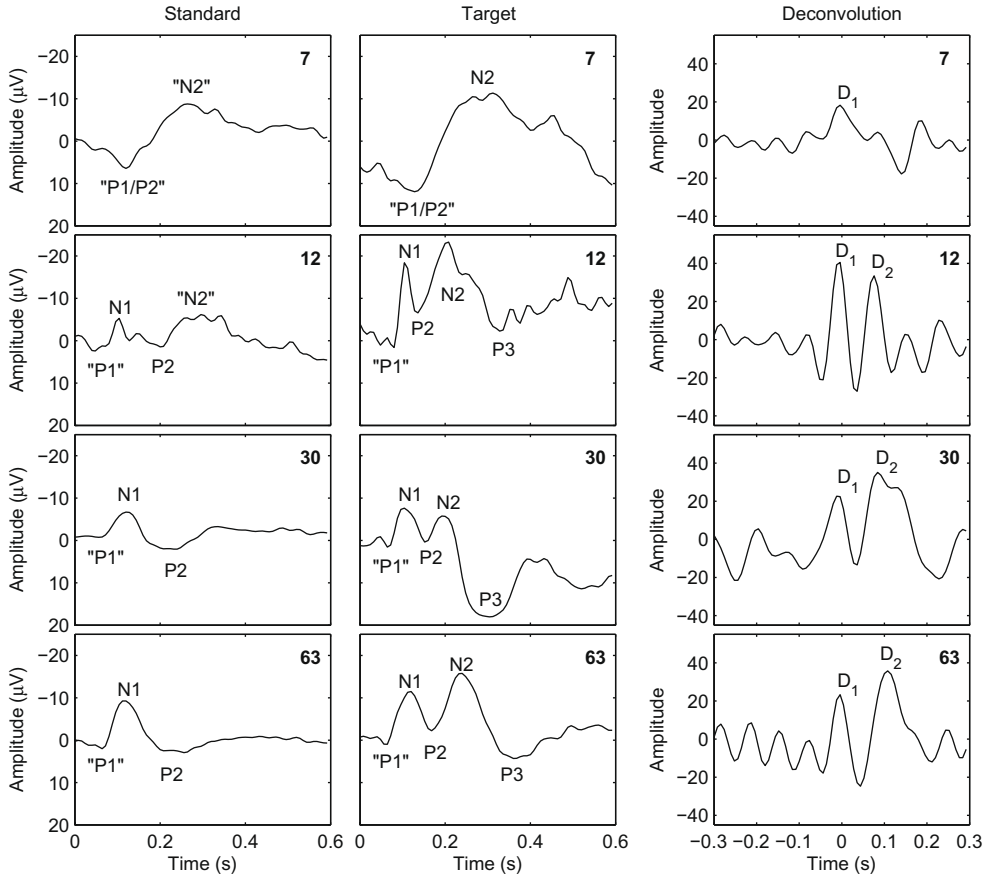

Fig. 1. Auditory evoked potentials recorded from the Cz electrode for standard (left column) and target (center column) stimuli, and analyzed using deconvolution (right column). Plots show single-subject responses at four characteristic ages: top row, 7 years; second row, 12 years; third row, 30 years; bottom row, 63 years. Adult AEP components (P1, N1, P2, N2, and P3) and deconvolution peaks (D_1 and D_2) are labeled. The AEPs of young children (top row) almost appear to be inverted with respect to those of adults, and typically yield a single deconvolution peak. AEP components that have been reported in other studies but are either not evident or not analyzed in these data are given in quotation marks.

3 ms/year (Brown et al., 1983), and some studies have found that the rate increases with age (Brown et al., 1983; Barajas, 1990). A second common finding is a decrease in P3 latency from childhood to adolescence. This decrease is much more rapid than the latency increase observed during aging, and has been reported to range from −5 ms/year (Johnstone et al., 1996; Oades et al., 1997) to −19 ms/year (Martin et al., 1988; Barajas, 1990). N2 displays latency trends that are similar to P3, though typically of smaller magnitude (Goodin et al., 1978; Fuchigami et al., 1993; Johnstone et al., 1996; Bahramali et al., 1999). Standard and target N1 and P2 also often show the same latency trends, though smaller in both absolute and relative magnitudes as compared to target N2 and P3 (Fuchigami et al., 1993; Johnstone et al., 1996; Albrecht et al., 2000; Ponton et al., 2002). In general, there is a correlation between the latency of a component and its rate of change, as reported by Goodin et al. (1978). This result suggests that the increases in latency are due to systemic causes, such as a uniform reduction in axonal transmission velocity, and is consistent with hypotheses of EEG and AEP generation involving long-range cortical and/or corticothalamic networks (Wright et al., 1990; Nunez, 1995; Rennie et al., 2002).

Compared to latencies, component amplitudes appear to have less pronounced age effects, and no changes in amplitude have been consistently reported. Amplitudes are considered to be more difficult to measure than latencies (Albrecht et al., 2000; Ponton et al., 2002), and they show less test-retest reliability (Segalowitz and Barnes, 1993). The most common findings are a decrease in P3 amplitude of up to −0.2 μV/year in adults (Dujardin et al., 1993), and an increase in target P2 amplitude of up to 0.5 μV/year in children (Johnstone et al., 1996).

Considerable changes in reaction time have been found during development, ranging from −50 ms/year between the ages of 4 and 8 (Fuchigami et al., 1993) to −15 ms/year between the ages of 8 and 17 (Johnstone et al., 1996). The elderly show no increase in reaction time compared to young adults in the oddball task, despite reporting greater task difficulty (Dujardin et al., 1993), although they do show an increase in reaction time when given difficult discrimination tasks, such as the semantic stimuli used by Tachibana et al. (1996). While not always the case (e.g., Kraiuhin et al., 1990), many authors have found correlations between reaction time and N2 or P3 latency (e.g., Goodin et al., 1978; Pfefferbaum et al., 1980; Polich, 1997)—a surprising result given that P3 latency shows a strong age trend while reaction time does not.

The changes in AEPs during development and aging can be linked to known changes in brain anatomy and physiology. These include the multi-stage development of the different cortical layers up to about age 12 (Ponton et al., 2002; Eggermont and Ponton, 2003), the 95% increase in myelination between birth and age 20 (Sowell et al., 2004), the gradual decline of myelination after age 40–50 (Miller et al., 1980; Piguet et al., 2007), synaptic pruning during development (Caviness et al., 1996), and gray matter density decreases during both development and aging (Peters, 2002; Sowell et al., 2004). While the

causative effects of most of these changes are speculative, their time courses are similar to the age ranges during which the most substantial changes in the AEP waveforms occur. Furthermore, some of these changes, such as the degree of myelination as an explanation of changes in latency, have a clear mechanism by which they could produce their effects.

Although analyses of AEPs in terms of component amplitudes and latencies do yield a number of interesting age trends, this type of analysis has severe limitations. First, it is difficult or impossible to apply in young children, whose waveforms show very different morphology from adults, and for whom the adult components as conventionally defined often do not exist, as shown in Fig. 1. Second, since components are *defined* by their latency and amplitude, arbitrary decisions about component classification are sometimes made when a waveform shows unusual morphology. Third, even if accurate component scores can be obtained, it is difficult to directly interpret changes in either amplitude or latency, since a change in one can cause a change in the other, due to the temporal overlap of adjacent components. Finally, it is not well understood what underlying physiology determines the amplitude and latency of AEP components.

To address these limitations of component scoring, this paper applies a recently-published method of evoked potential (EP) deconvolution to gain further insight into the physiology underlying EP age trends (Kerr et al., 2009). Deconvolution is based on the observation that standard and target responses have both similarities (e.g., N1) and dissimilarities (e.g., N2), and is thus more similar in motivation to the calculation of a difference waveform, such as mismatch negativity (Kerr et al., 2009), than it is to conventional deconvolution techniques, which either aim to separate overlapping responses (Woldorff, 1993; Özdamar and Bohórquez, 2006; Wang et al., 2006), or function as alternatives to ensemble averaging (Ungan and Başar, 1976; Wastell, 1981). However, unlike the difference waveform, deconvolution allows a wide variety of similarities to be removed from the target response, including time-shifted and amplitude-scaled versions of the standard response. Deconvolution has been shown to be applicable to both single-subject and group average AEP time series, and yields quantifications that have less variance than corresponding measures based on component scoring (Kerr et al., 2009).

A further limitation of most previous papers on AEP age trends is the regression method used to describe the data. Previous work has used either (i) a single linear fit (e.g., Polich, 1997), (ii) two or more linear fits (e.g., Goodin et al., 1978), (iii) a second-order polynomial fit (e.g., Anderer et al., 1996), or (iv) an exponential fit (e.g., Ponton et al., 2002). However, each of these methods has severe limitations. Methods (i) and (iv) can describe changes occurring during development or aging, but not over the entire age range. Method (ii) relies on the unrealistic assumption of a discontinuous change in slope, whereas age trends are almost certainly smooth. Method (iii) may accurately describe certain aspects of the data, but is unable to fit linear regions. It also requires symmetry around the turning point, whereas the data show strong trends during development (ages 6–20), a period of negligible change during intermediate ages (ages 20–40), and moderate change during aging (ages 40–86). Hence, none of these methods result in fits that are biologically plausible, and here we present a new fitting method to overcome these limitations.

The remainder of this paper is organized as follows. Section 2 describes the experimental data and analysis methods used in the study. Section 3 describes the effects of development and aging on the AEP time series, component scores, deconvolution time series, and deconvolution peak quantifications. Section 4 compares the results of component scoring and deconvolution, and discusses their possible physiological interpretations.

2. Methods

2.1. Experimental data

Auditory oddball EPs were recorded from 1498 subjects (763 males, 735 females) with an age range of 6.1–86.6 years, as shown in Fig. 2. The subjects comprised the 1008 used by Williams et al. (2008) in a wide-ranging multi-modal study of aging, plus 490 more recently acquired subjects. All subjects were healthy, and reported no history of brain injury, disease, or other medical conditions that could influence the normality of the EEG (van Albada et al., 2007). Data collection was done by Brain Resource Ltd. (Ultimo, NSW, Australia; www.brainresource.com) and results were made available through the Brain Resource International Database (BRID) (Gordon et al., 2005).

Recordings were made at 26 electrode sites from an extension to the International 10–20 system, following previously published methods for acquisition and artifact removal (Rowe et al., 2004; Gordon et al., 2005). EEG data were recorded at a 500 Hz sampling rate and an A/D precision of 0.06 μV through a NuAmps (Neuroscan) amplifier using an averaged mastoid reference and a low-pass third-order Butterworth filter with a −6 dB point at 50 Hz.

Subjects were presented binaurally, via headphones, with a series of standard and target tones (500 and 1000 Hz, respectively), at 75 dB SPL and lasting for 50 ms, with a constant ISI of 1 s. Subjects were instructed to ignore standard tones, but to respond to target tones with a button press. There were 280 standard (82%) and 60 target (18%) tones presented in pseudorandom order, with the only constraint being that two targets could not appear consecutively. Total task duration was 6 min. EEG data were corrected offline for eye movements according to a method based on that of Gratton et al. (1983). AEP data were extracted from EEG recordings by averaging over a window from 0 to 0.6 s relative to stimulus onset. Target and standard responses were averaged separately.

2.2. Component scoring

Scoring of the amplitude and latency of each component of the target and standard EPs was performed by Brain Resource Ltd.

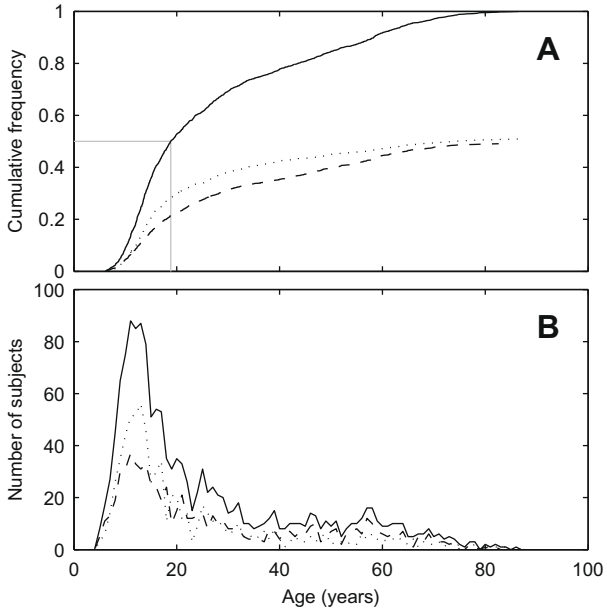

Fig. 2. (A) Cumulative distribution function and (B) density distribution function (with one-year age bins) for all subjects across age (solid lines). Separate distribution functions for females (dashed lines) and males (dotted lines) are also shown. The distribution of subjects is skewed towards young ages, such that more than half of all subjects were under age 20 (A, gray line).

using an automated system (Haig et al., 1995). Components were scored as either the most negative (N) or most positive (P) extremum in the following latency ranges: N1, 80–140 ms; P2, 150–200 ms; N2, 205–290 ms; P3, 280–550 ms. P1 was not scored, and P3 was scored only if it was not a result of EOG contamination (as seen in the EOG channel). Amplitudes were measured relative to a pre-stimulus (200 ms duration) baseline. If automated AEP scoring was judged by trained operators to be incorrect (10% of data), manual scoring of components was undertaken.

2.3. Deconvolution

Deconvolution analysis of AEPs was performed according to the method developed by Kerr et al. (2009), which we summarize here. The motivation for this approach comes from the fact that standard and target AEPs have a large degree of overlap in the information they contain, as evidenced by the strong correlations typically found between component scores (Fuchigami et al., 1993). The aim of deconvolution is to remove as much of this redundancy as possible. As shown schematically in Fig. 3, conventional deconvolution techniques (e.g., Hansen, 1983; Jewett et al., 2004; Özdamar and Bohórquez, 2006), use a known sequence of impulses to recover the impulse response function. In contrast, here the impulse response function is assumed to be the standard response, allowing the sequence of impulses to be recovered.

Since it is unlikely that targets result from a literal superposition of standard waveforms, the sequence of impulses obtained using deconvolution needs to be interpreted in terms of a physiological framework. The physiological basis for deconvolution has yet to be investigated using independent experimental methods; however, as described in Section 4.3, a plausible hypothesis for the observed results is the sequential activation of cortical networks by impulses from the thalamus (Kerr et al., 2009).

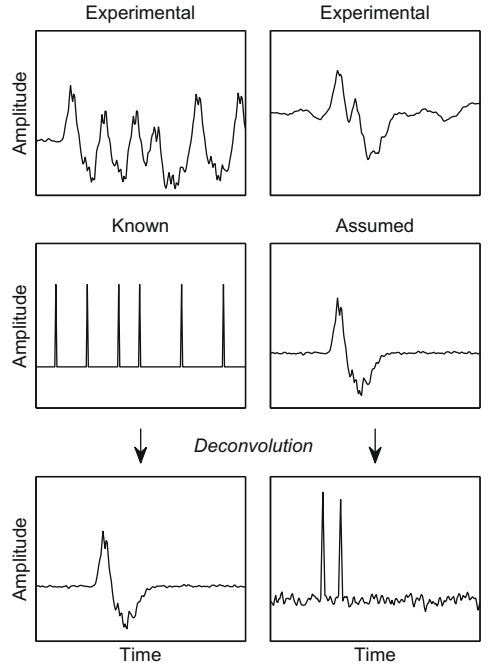

Fig. 3. Comparison of conventional deconvolution methods (left) with the method used here (right). In conventional deconvolution, the experimental waveform (top) is deconvolved using a known sequence of impulses (middle), resulting in an underlying waveform (bottom). In the method used here, the experimental waveform (the target response, top) is deconvolved using an assumed underlying waveform (the standard response, middle), yielding a sequence of impulses (bottom).

The deconvolution method hypothesizes that each AEP time series is a convolution of a task-dependent function (which changes between standards and targets) and a task-invariant function (which does not):

$$R_S(t) = D_S(t) \otimes I(t) + N_S(t), \tag{1}$$

$$R_T(t) = D_T(t) \otimes I(t) + N_T(t), \tag{2}$$

where $\otimes$ represents convolution; R_S and R_T are the standard and target responses, respectively; D_S and D_T are task-dependent functions for standards and targets, respectively; I is the task-invariant function; and N_S and N_T are noise in the target and standard, respectively.

To eliminate the task-invariant function, we first Fourier transform Eqs. (1) and (2), obtaining

$$\widetilde{R}_S(\omega) = \mathscr{F}[R_S(t)] = \widetilde{D}_S(\omega)\widetilde{I}(\omega) + \widetilde{N}_S(\omega), \tag{3}$$

$$\widetilde{R}_T(\omega) = \mathscr{F}[R_T(t)] = \widetilde{D}_T(\omega)\widetilde{I}(\omega) + \widetilde{N}_T(\omega), \tag{4}$$

where $\mathscr{F}$ denotes a Fourier transform, ω is angular frequency, and tildes denote frequency-domain functions. We then take the ratio of Eqs. (4) and (3), and apply a Wiener filter (Wiener, 1949; Kerr et al., 2009) to attenuate noise:

$$\widetilde{D}_C(\omega) = \frac{\widetilde{R}_T}{\widetilde{R}_S}\left[\frac{|\widetilde{R}_S|^2}{|\widetilde{R}_S|^2 + NSR}\right], \tag{5}$$

where $\widetilde{D}_C$ represents the change in the brain's task-dependent properties between target and standard responses, the term in brackets is the Wiener filter, and NSR is the noise-to-signal ratio, defined as

$$NSR(\omega) = \left|\frac{\alpha\omega^{-1}}{e^{-\sigma^2\omega^2}}\right|^2, \tag{6}$$

where the numerator is the noise in the target and the denominator is the signal we are expecting to find. This form of NSR was chosen since the amplitude of the noise in the target is approximately inversely proportional to frequency, and since the signal may conservatively be chosen to be a Gaussian impulse (Kerr et al., 2009). The constant α was chosen so $NSR(10\,\text{Hz}) \approx 1$, and σ was chosen to be 10 ms, as these provided the best empirical results.

Finally, an inverse Fourier transform completes the deconvolution:

$$D_C(t) = \mathscr{F}^{-1}[\widetilde{D}_C(\omega)]. \tag{7}$$

All differences between the target and standard responses are contained in the deconvolution D_C. Since D_C is produced by an inverse Fourier transform, it is a periodic function, with a period equal to the length of the original time series.

The latency of a peak in D_C corresponds to the *relative response latency* between standards and targets. For example, if a feature occurs with the same latency in both waveforms, then it will produce a peak in D_C with zero latency; a feature that appears in targets earlier than in standards will result in a peak in D_C with negative latency. Peak latency can be easily and accurately quantified by inspection or by an automated algorithm, since peaks in D_C are usually narrow and symmetric.

Peak area corresponds to *relative response amplitude*, so a feature with identical amplitude in standards and targets will produce a peak in D_C of unit area. Hence, if standard and target waveforms are identical, then deconvolution will yield a single peak with zero latency and unit area. In general, target features have larger amplitude than standards, so peak area is usually greater than one. Peak area can be calculated by

$$\mathscr{A} = \mathscr{N}\int_{t_a}^{t_b} D_C(t)\mathrm{d}t, \tag{8}$$

where $\mathscr{A}$ is the peak area, t_a and t_b are the times at which D_C returns to zero on either side of the peak, and $\mathscr{N}$ is a normalization coefficient, given by

$$\mathscr{N} = \frac{\int_{-\infty}^{\infty} |\widetilde{D}'_C \widetilde{D}_C| \mathrm{d}\omega}{\int_{-\infty}^{\infty} |\widetilde{D}_C|^2 \mathrm{d}\omega}, \tag{9}$$

where $\widetilde{D}_C$ is the Wiener-filtered deconvolution spectrum and $\widetilde{D}'_C$ is the spectrum prior to filtering. This normalization coefficient ensures that Wiener filtering does not change the total power of D_C.

2.4. Regression analysis

To obtain lines of best fit for the age trends, we first made the following observations: (i) most measures showed highly non-normal distributions, motivating the use of median- rather than mean-based fitting methods; (ii) the median often shows approximately linear trends at very young and very old ages; (iii) the ages at which these linear trends become nonlinear vary substantially; (iv) in most cases there is a gradual transition from a "development" trend to an "aging" trend, often with a period of little change during middle age; and (v) in no cases did the median clearly show more than one turning point. This motivated the choice of a fitting function that is smooth, asymptotically linear, and has a second derivative of constant sign. A function that meets these requirements is given by

$$y = Cx + \tau(C - A) \ln\left(1 + \exp\left[\frac{I - x}{\tau}\right]\right) + D, \tag{10}$$

$$I = \frac{B - D}{C - A}, \tag{11}$$

where x is the age, τ is the characteristic width of the nonlinear transition region, and A, B, C, and D are fitted parameters. As $x \to -\infty$, Eq. (10) simplifies to $y = Ax + B$, while it simplifies to $y = Cx + D$ as $x \to \infty$. Hence, Eq. (10) simply describes a smooth interpolation between two straight lines that intersect at age I, as shown in Fig. 4. The fits are relatively insensitive to the parameter τ, and hence τ was fixed at three years, as this yielded sufficiently good fits to the data. Since the parameters A and C are the slopes of the fitted trend at the "ages" $-\infty$ and ∞, respectively, we instead report a "development" slope (the slope of fitted trend at age 6) and an "aging" slope (the slope of the fitted trend at age 86). Although the difference between C and the slope at age 86 is usually negligible ($\ll 1\%$), there can be a difference of more than a factor of two between A and the slope at age 6.

In order to track the median rather than the mean, fits were performed by minimizing the mean absolute difference, rather than squared deviations, between fitted and measured values. Optimization was achieved using a downhill simplex method (Nelder and Mead, 1965), with starting conditions obtained by linear least-squares fits to subjects aged 6–15 and 40–86. Confidence intervals and standard errors for the parameters and fits were obtained by bootstrapping with 1000 resamplings.

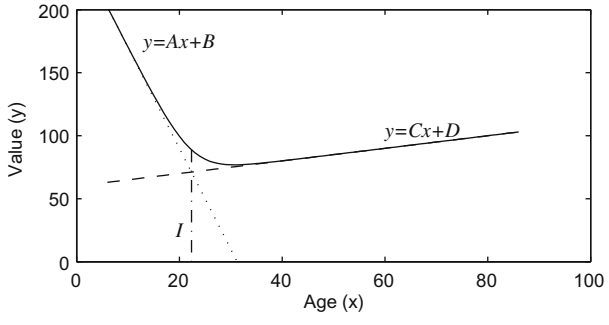

Fig. 4. Schematic diagram of the fitting function used to provide lines of best fit for age trends (solid line). Age trends are often approximately linear at young and old ages, and in these regions, the fitting function asymptotes to the linear functions $y = Ax + B$ (dotted) and $y = Cx + D$ (dashed), respectively. The two linear functions intersect at age $x = I$ (dash-dotted), which is also the age at which the slope of the fitting function changes most rapidly.

3. Results

This section describes the qualitative changes in the AEP and deconvolution time series across age, and quantifies these results in terms of conventional component scores and deconvolution peak areas and latencies. Data from several midline electrodes (Fz, Cz, and Pz) are shown in Figs. 5 and 8, and presented in Table 1, demonstrating a general consistency of age trends across the scalp. Since a full analysis of the spatial variation in age trends is beyond the scope of this study, and since the age trends at Cz appear to be representative of those at other midline sites, subsequent analysis and discussion will focus on Cz data, unless otherwise noted.

3.1. Time series

Age trends are clearly evident from contour plots of the time series data versus age, shown in Fig. 5. Due to the large degree of inter-subject variability, these plots (and the comparable plots for the deconvolution time series, Fig. 8) show average waveforms for bins of subjects moving across age.

Changes occured most rapidly during development, and adult forms of the responses were reached by approximately age 15. For both standards and targets, in adults the first deflection (N1) was negative, and the second (P2) was positive. By contrast, young children (< 10 years) appeared to show an "inverted" response, such that a positive deflection preceded a negative one. Since there is no objective method for adapting scoring rules to waveforms with different morphologies, using adult component definitions to assign components in young children will produce erroneous results, such as discontinuities with age as the waveform approaches adult morphology.

The positive component of latency 100–150 ms in young children showed similar age trends in standards and targets, with a negativity appearing at approximately age 9 that was continuous with the adult N1 component. However, inspection of single-subject waveforms showed that this negativity is already present in some target responses by age 6, which explains why the amplitude of the positive component is larger in standards than in targets, such that it is not clearly visible in the group average target waveform beyond age 7. The negative component of latency ~ 250 ms in young children disappeared in standards during age 10–12, and appeared to merge with N2 in targets. The time course of target P3 development is difficult to discern from Fig. 5D, as significant variability remained even when averaged over 30 subjects. However, this component appeared to emerge between ages 9 and 10, and did not reach maximum amplitude until the mid-twenties as shown in Fig. 5B.

Age-related changes in amplitude were visible in all components during adulthood: small increases in the magnitudes of standard N1 and target N1, a large decrease in the magnitude of target P3, increases in the magnitudes of standard P2 and target P2, and an increase followed by a decrease in the magnitude of target N2. Target N2 and P3 latencies decreased during development and increased during aging, but no other components showed obvious latency changes.

3.2. Component scores

All component scores showed at least one statistically significant age trend, as shown in Fig. 6 and Table 1. "Development"

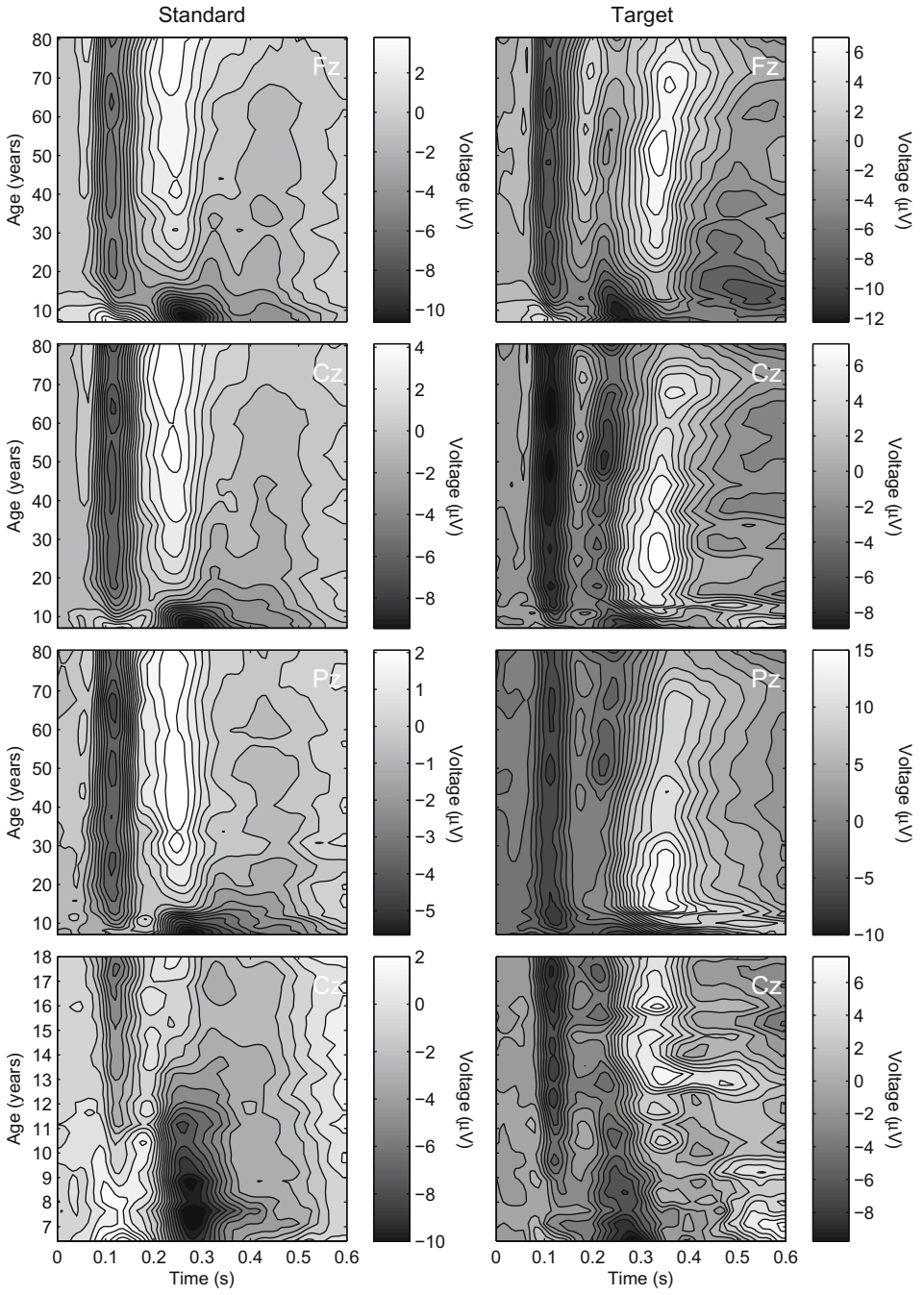

Fig. 5. Age trends in AEPs, showing scalp potential (shading) as a function of time from stimulus presentation (horizontal axes) and subject age (vertical axes). Rows 1–3 show standard (left) and target (right) AEPs for electrodes Fz, Cz and Pz. Waveforms are plotted using moving average age bins. Since changes occur more rapidly during development, and since more subjects were available at young ages, narrow age bins (2 years) were used below age 14, and bin width was increased with increasing age, up to a maximum width of 8 years for subjects over 40. The bottom row is a magnified view of the developmental changes in standard and target AEPs at Cz, plotted using a moving average age bin of width 0.8 years.

age trends were significant for all component amplitudes, and all component latencies except standard N1. In addition to these age trends in median values, the variances of component scores also showed significant age effects. For example, the standard deviation of standard N1 latency changed from 37 ms for subjects under 10 to 12 ms for subjects over 20, a difference that is highly significant ($p < 10^{-6}$, Levene's test). In fact, children showed greater latency variance than adults for all components except standard P2 with significances of $p < 0.003$. However, latency variance reduced rapidly with age, and children older than 12 no longer showed statistically significant differences with adults ($p > 0.5$). Since AEP waveforms show more variance in adults than young children (Bishop et al., 2007), the large variances in the component latencies of children under 12 appear to be due to problems with applying adult component definitions to these subjects.

Furthermore, the amplitude of the standard N1 component in children under age 7 was not statistically different from zero ($p = 0.3$, Wilcoxon signed-rank test). Visual inspection of single-subject waveforms corroborates this result, indicating that the N1 component is absent in a significant fraction of children under age 7. Indeed, the only components that appear to be present in both young children in adults, as evidenced by Fig. 5, are target

Table 1
Age trends in the amplitudes and latencies of each AEP component (S, standard; T, target) for electrodes Fz, Cz, and Pz. Values give the slopes of the lines of best fit shown in Fig. 6 at age 6 ("development") and age 86 ("aging"); standard errors are also shown. Slopes that differ from zero by more than two standard errors are shown in bold.

		Amplitude change (μV/year)		Latency change (ms/year)	
Site	Component	Development	Aging	Development	Aging
Fz	S–N1	**−1.0 ± 0.3**	−0.007 ± 0.007	5 ± 14	**−0.27 ± 0.09**
	S–P2	**−1.4 ± 0.2**	**0.100 ± 0.005**	**9 ± 1**	**−0.040 ± 0.006**
	T–N1	**−0.6 ± 0.3**	−0.01 ± 0.02	**−0.6 ± 0.2**	−0.02 ± 0.04
	T–P2	**−0.7 ± 0.3**	**0.08 ± 0.02**	**7 ± 3**	**−0.08 ± 0.03**
	T–N2	**0.54 ± 0.09**	**0.017 ± 0.004**	**−3 ± 1**	**0.4 ± 0.1**
	T–P3	**0.28 ± 0.03**	**−0.07 ± 0.02**	**−18 ± 4**	**0.51 ± 0.09**
Cz	S–N1	**−0.7 ± 0.1**	−0.007 ± 0.006	5 ± 3	**−0.14 ± 0.03**
	S–P2	**−0.9 ± 0.2**	**0.075 ± 0.007**	**8 ± 1**	**−0.23 ± 0.03**
	T–N1	**−0.8 ± 0.4**	−0.01 ± 0.01	**−0.4 ± 0.1**	**0.08 ± 0.03**
	T–P2	**−0.6 ± 0.2**	**0.05 ± 0.01**	**−1.9 ± 0.7**	−0.04 ± 0.04
	T–N2	**3 ± 1**	−0.03 ± 0.02	**−5 ± 1**	**0.63 ± 0.07**
	T–P3	**0.8 ± 0.2**	**−0.07 ± 0.02**	**−19 ± 3**	**0.6 ± 0.1**
Pz	S–N1	**−0.6 ± 0.3**	−0.006 ± 0.005	4 ± 1	−0.04 ± 0.04
	S–P2	**−0.13 ± 0.06**	**0.033 ± 0.005**	**8.5 ± 0.8**	**−0.11 ± 0.02**
	T–N1	−0.7 ± 0.5	**0.023 ± 0.008**	−0.4 ± 0.2	0.06 ± 0.04
	T–P2	0.0 ± 0.8	**0.05 ± 0.02**	−3 ± 3	−0.17 ± 0.05
	T–N2	**2.2 ± 0.7**	**−0.06 ± 0.02**	**−4.8 ± 0.6**	**0.46 ± 0.08**
	T–P3	**1.2 ± 0.2**	**−0.13 ± 0.03**	**−16 ± 2**	**0.6 ± 0.1**

N2 and P3, both of which decrease considerably in latency during development (−5 and −19 ms/year, respectively).

One of the strongest age trends in Fig. 6 is the increase in standard P2 latency of 8 ms/year during development, but comparison with Fig. 5 suggests that this latency increase is a consequence of the disappearance of the 250 ms negativity and the concurrent emergence of N1. It is instructive that the most statistically robust latency age trend observed using component scoring is in fact an illusion, caused by changes in the amplitudes of two unrelated components.

While superposition of adjacent components is also an important consideration in the interpretation of component age trends in adults, the changes to the AEP time series during aging evident in Fig. 5 are mostly captured by scoring. Significant changes in amplitude were observed only in the positive components, with standard and target P2 increasing in amplitude (0.075 and 0.05 μV/year, respectively), and target P3 decreasing (−0.07 μV/year). Small but significant latency changes were observed for standard P2 and standard and target N1 components during aging, although these changes are not visible in Fig. 5. Target N2 and P3 both showed considerable latency increases during aging (0.6 ms/year).

In addition, numerous correlations were found between component scores, as shown in Fig. 7. Interestingly, although a wide range of correlations was observed at all latencies, the upper bound (the maximum correlation at a given latency difference) did appear well defined, especially for adults (age > 20 years). Most of the points that define the upper bound are correlations between the amplitudes of different target components, although the highest correlation was found between target and standard N1 amplitudes. Due to the small number of data points, the upper bound in adults can be described almost equally well as either a linear decrease (with a slope of $-2.6\ s^{-1}$, $r^2 = 0.99$) or as an exponential decay (with a time constant of 150 ms, $r^2 = 0.98$). However, the upper bound in young subjects (age < 20 years) could not be described by either linear or exponential forms ($r^2 = 0.53$ and 0.54, respectively).

3.3. Deconvolution

The high degree of correlation between components indicates that a significant amount of information is shared between them; deconvolution removes much of this shared information, allowing the underlying salient features to be determined. As shown in Fig. 8, the deconvolution time series contains many fewer features than the original AEP waveforms (Fig. 5). Below age 10, the deconvolution time series contains a single narrow peak with latency of approximately 0 ms and unit area. This corresponds to standard and target waveforms being nearly identical, and indicates that young children have similar neurophysiological responses to target and standard stimuli, as shown in Fig. 1. However, an additional peak appeared between the ages of 10 and 15, corresponding to improved differentiation between the two types of stimuli. While the first peak in the deconvolution time series ("D_1") remained almost unchanged over eight decades of life (no significant development or aging trends were observed), the second peak ("D_2") increased in latency and decreased slightly in amplitude during aging. Note that the periodic peaks (e.g., at −200 and −100 ms) and troughs (e.g., at ±50 ms) are a "ringing" artifact resulting from the low-pass characteristics of Wiener filtering. However, the presence of features at negative time is not in itself impossible: it simply implies that a feature occurs earlier in targets than in standards.

Quantification of the two features present in the deconvolution time series closely matches qualitative inspection of Fig. 8. Age trends in the amplitude and latency of these features are shown in Fig. 9, with the slopes and significances of the lines of best fit given in Table 2. No significant trends were observed in either the amplitude or latency of the first peak: throughout the age range its amplitude is approximately one, and its latency is approximately zero. This indicates that the initial processing of targets is virtually identical to that of standards, irrespective of age.

In contrast to the constancy of the first peak, the second peak began with an area of near zero at age 6, and increased rapidly to a near-adult value of 1.5 by age 15. The latency of the second peak decreased during development, although this trend was not as strong as that in target N2 or P3, since the peak is often too small for an accurate latency measurement to be made. The increase in the latency of the second peak during aging was equal to the latency change in the target N2 or P3 components to within statistical uncertainty. Thus, deconvolution captures the most important aging trend in component scores—the increase in latency with age—and describes the process of development as a process of improved differentiation between standards and targets.

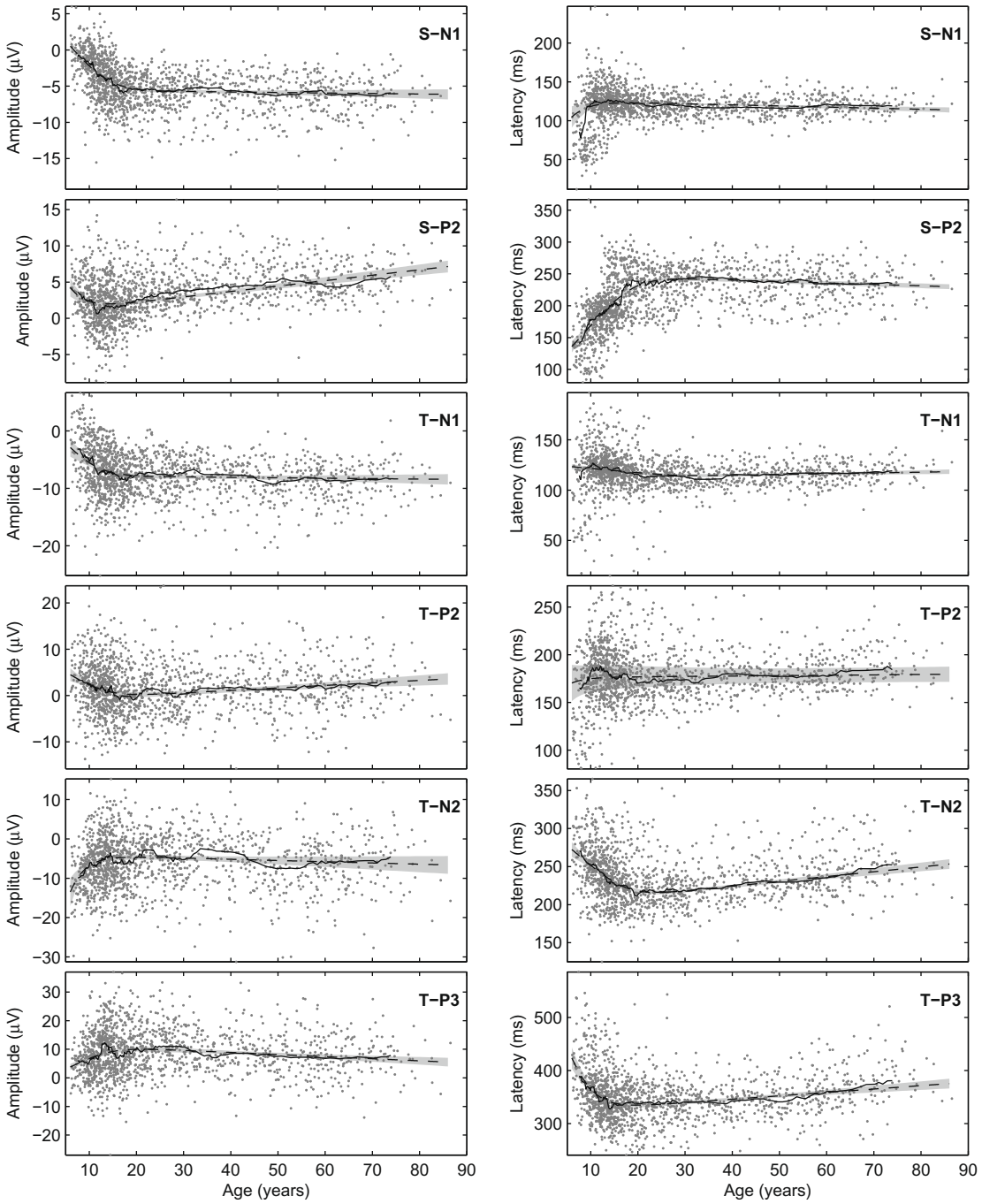

Fig. 6. Age trends in the amplitudes (left column) and latencies (right column) of individual AEP components (S, standard; T, target), showing scores for each subject (gray dots), lines of best fit (dashed lines), moving medians (solid lines), and 95% confidence intervals (shaded regions). Line slopes and their significances are given in Table 1.

3.4. Reaction time and error rate

As shown in Fig. 10, reaction time decreased considerably during development, at a rate of -50 ± 15 ms/year. It appeared to reach a minimum at approximately age 18, and increased slightly thereafter, but this change was not statistically significant. The error rate, defined as the number of times the subject responded to standard stimuli (type I errors) plus the number of times the subject failed to respond to target stimuli (type II errors), was seen to decrease with age during development (-0.4 errors/year) but underwent no further change, since the majority (60%) of subjects over age 15 made no errors during the task.

The correlations between reaction time and AEP measures (component scores and deconvolution peak quantifications) are shown in Table 3. The presence of nonlinear age trends in the data precludes the use of either a direct correlation or a partial correlation corrected for age. Hence, we present correlations between age trends (as determined by the lines of best fit), as well as correlations between the residuals once these age trends have been removed. The correlations between age trends indicate the degree to which the two measures have the same time course and relative amplitude of developmental and aging slopes. The correlations between residuals indicate the degree to which the two measures are correlated within individual subjects.

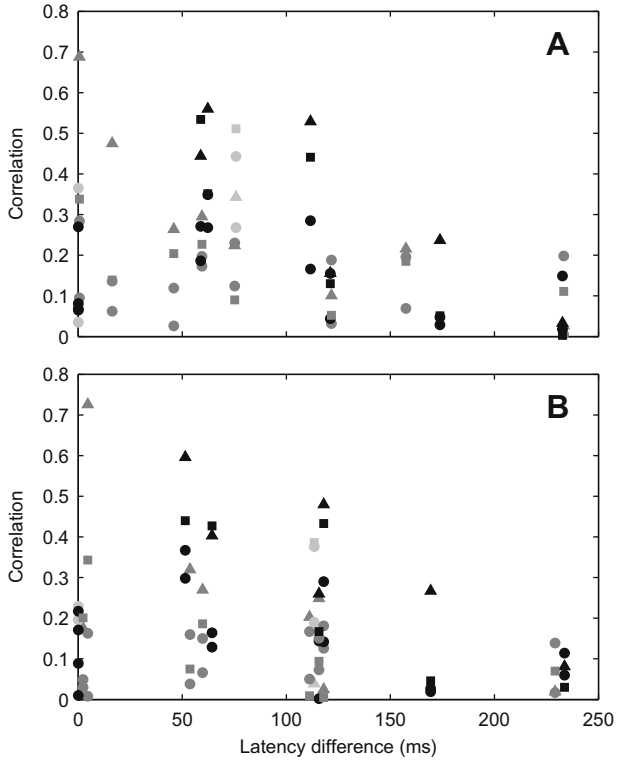

Fig. 7. The correlation strengths between different AEP component scores, as a function of mean latency difference between them, for (A) subjects under 20 years of age, and (B) subjects over 20 years of age. Shape denotes component score type (triangles: amplitude–amplitude; circles: amplitude–latency; squares: latency–latency), and color denotes AEP type (light gray: standard–standard; dark gray: standard–target; black: target–target). In both age ranges, the strongest correlation is between standard and target N1 amplitudes.

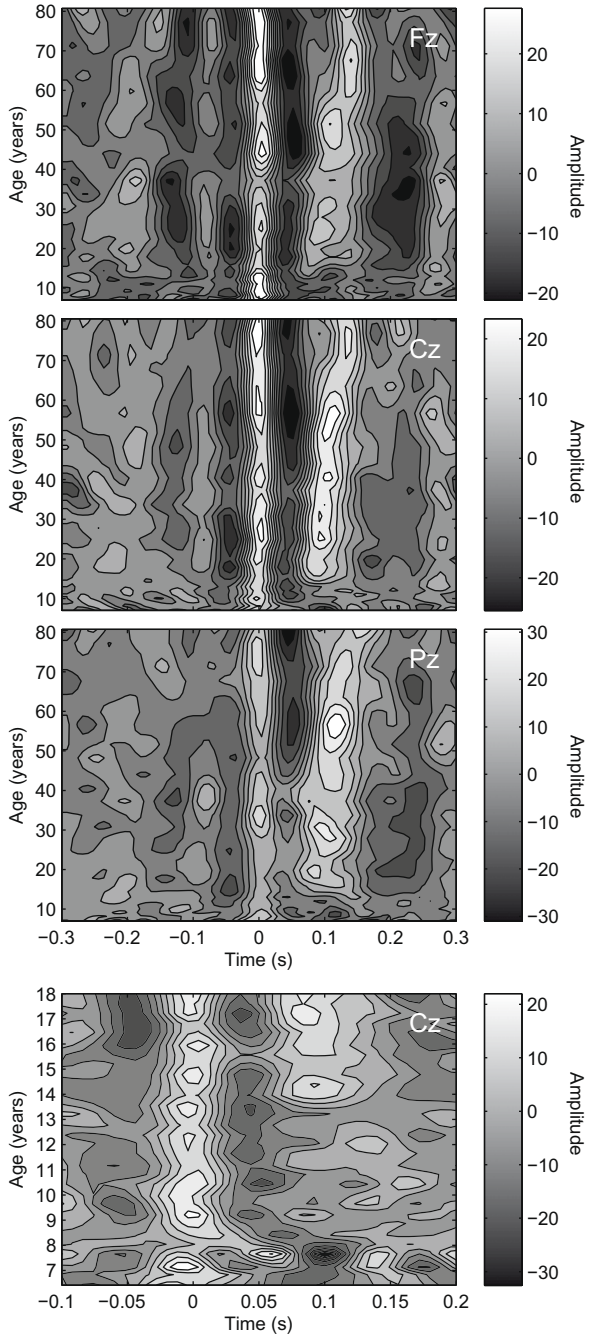

Fig. 8. Age trends in the deconvolution time series, showing its unitless amplitude (shading) as a function of time (horizontal axes) and subject age (vertical axes). The upper three plots show the deconvolution time series for electrodes Fz, Cz, and Pz, respectively, plotted using moving average age bins with widths varying from 2 years (for subjects < 14) to 8 years (for subjects > 40). The bottom plot is a magnified view of developmental changes at Cz, plotted using a moving average age bin of width 0.8 years. The presence of a feature with latency ~ 0 ms at all ages indicates that target AEPs always contain a standard-like response. The appearance during adolescence of a second feature with latency ~ 100 ms corresponds to a second (time-shifted, amplitude-scaled) standard-like response in the target waveform. The oscillatory feature visible at negative time in adults is an artifact caused by the low-pass characteristics of the Wiener noise filter.

Highly statistically significant correlations in age trends were found between reaction time and all AEP-based measures ($p < 10^{-9}$ in all cases), since both reaction time and AEP measures show changes of slope at relatively young ages (under 30), and since both show stronger trends during development than aging. The strongest correlations were between reaction time and standard P2 latency ($\rho = -0.96$), D_2 peak area ($\rho = -0.95$), and target N1 amplitude ($\rho = -0.92$).

Correlations between residuals were very small, with standard P2 latency ($\rho = -0.16, p < 10^{-6}$), standard N1 amplitude ($\rho = 0.13$, $p < 10^{-4}$), and target N2 amplitude ($\rho = 0.13, p < 10^{-4}$) being the most significant. Residuals for target P2 and N2 latency also showed significant correlations with reaction time ($\rho = 0.11, p < 10^{-3}$), but target P3 latency residuals did not. Residuals for D_2 peak area and D_1 peak latency showed significant correlations with reaction time ($\rho = -0.07$, $p < 0.05$ and $\rho = 0.06$, $p < 0.05$, respectively).

Error rate was typically correlated with the same AEP measures as reaction time, but the magnitudes of these correlations were smaller; the only significant correlation for error rate residuals was with reaction time ($\rho = -0.1$, $p = 0.003$). Age trends in reaction time and error rate show a strong positive correlation ($\rho = 0.9, p < 10^{-9}$), since both improve markedly during development.

3.5. Sex differences

No significant differences were found in age trend slopes when male and female groups were compared. However, males and females did have significantly different means for some measures at some ages, as shown in Fig. 11. During adulthood, women had significantly shorter latencies for three components (standard N1, standard P2, and target P3) and significantly longer reaction times than men, as listed in Table 4. Several other measures also showed significant differences over more limited age ranges; for example, target P2, N2, and P3 amplitudes were more positive in females than males over the age range 40–60.

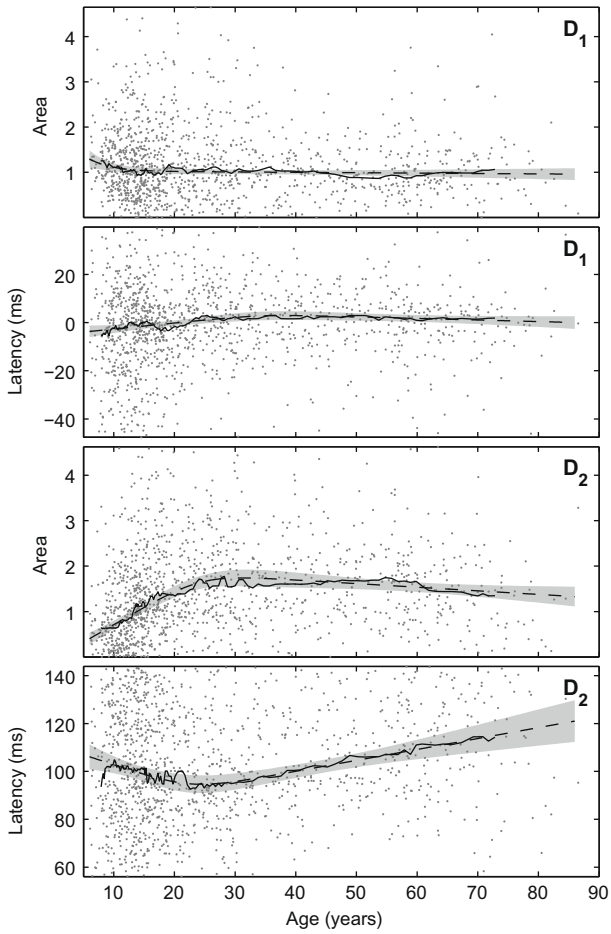

Fig. 9. Age trends in the areas and latencies of the deconvolution peaks D_1 and D_2, showing values for each subject (gray dots), lines of best fit (dashed lines), moving medians (solid lines), and 95% confidence intervals (shaded regions). Line slopes and their significances are given in Table 2. The first peak shows no significant change in either area or latency with age, while the second peak shows significant changes in area and latency during both development and aging.

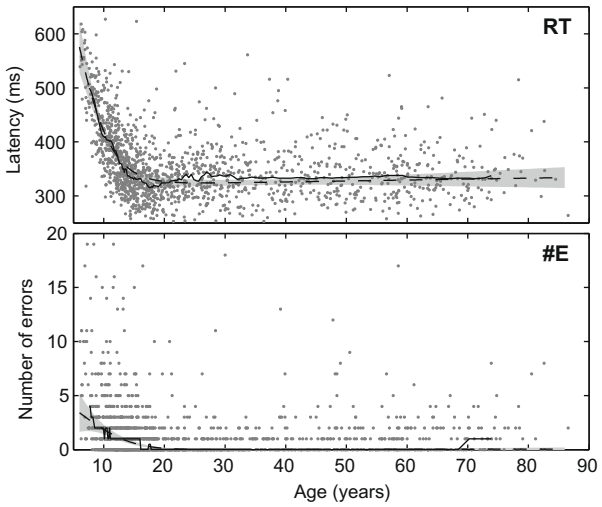

Fig. 10. Age trends in reaction time (RT) and error rate (#E), showing values for each subject (gray dots), lines of best fit (dashed lines), moving medians (solid lines), and 95% confidence intervals (shaded regions). Line slopes and their significances are given in the text.

4. Discussion

This study has examined the results of applying component scoring and deconvolution methods to AEP age trends obtained from a database of 1498 healthy subjects. Significant trends during development and/or aging were observed in all component scores. Scores that had significant trends over both age ranges showed greater rates of change during development than during aging, and the total change over the course of development (ages 6–20) was greater than the total change during aging (ages 40–86). In contrast to component scoring, which yielded 19 statistically significant age trends, deconvolution yielded four, of which only two were highly significant ($p < 0.01$). However, these two age trends—an increase in the amplitude of D_2 during development, and an increase in its latency during aging—appear to capture much of the information contained in the highly redundant component score age trends. Hence, deconvolution presents a much simpler view of development and aging, and reveals the developmental changes associated with improved ability to distinguish between target and standard stimuli.

In contrast to previous authors, who have used mostly piecewise linear or second-order polynomial fits to age trend data, we have introduced a regression formula (Eq. 10) that is biologically plausible, since it is smooth and allows for asymmetric age trends. A further advantage of this method is that the parameters are easily interpretable, since they correspond to asymptotically linear trends.

Table 2
Age trends in the areas and latencies of the deconvolution peaks D_1 and D_2. Values give the slopes of the lines of best fit shown in Fig. 9 at age 6 ("development") and age 86 ("aging"); standard errors are also shown. Slopes that differ from zero by more than two standard errors are shown in bold.

	Area change (per year)		Latency change (ms/year)	
Peak	Development	Aging	Development	Aging
D_1	−0.07 ± 0.04	−0.001 ± 0.003	0.25 ± 0.14	−0.07 ± 0.04
D_2	**0.08 ± 0.01**	**−0.008 ± 0.004**	**−0.8 ± 0.3**	**0.5 ± 0.1**

4.1. Morphology

Perhaps the most interesting change in AEPs with age is the amplitude "inversion" that occurs between the ages of 6 and 15. At age 6, both the standard and target responses of most subjects display an initial positivity with a latency of 100–150 ms, followed by a negativity with a latency of 250–300 ms. By age 15, however, the most prominent early component in both responses is a negativity with a latency of roughly 100 ms (N1). Standard and target responses also differentiate during development, resulting in the presence of N2 and P3 components in the target and their absence in the standard. Target responses appear to reach adult morphology at an earlier age than standard responses, suggesting that the neural pathways associated with attentional processing complete development before those that deal with inhibiting extraneous stimuli.

It has been argued that the 100–150 ms latency positivity in young children corresponds to adult P1, P2, or both (Ponton et al., 2000; Ponton et al., 2002; Eggermont and Ponton, 2003). However, our results suggest a more cautious interpretation of the time course of this feature. The component scoring method used here scored this feature as P2, and yielded a significant increase in its latency during development. This is in stark contrast to all other components, which showed either no change or decreases in latency. Additionally, P2 amplitude decreased substantially during the same period. These results suggest that the positivity with latency ~ 200 ms clearly present after adolescence

Table 3
Spearman correlations between reaction time and other measures, in terms of correlations between their age trends, as well as correlations between residuals once these age trends have been subtracted. Both component scores and deconvolution peak quantifications are listed (S, standard; T, target; D, deconvolution). For scoring measures, the "Size" column refers to peak amplitude; for deconvolution, it refers to peak area. Statistically significant correlations between residuals ($p < 0.05$) are marked with asterisks, and their p values are given.

	Size			Latency		
Measure	Age trends	Residuals	p	Age trends	Residuals	p
S–N1	0.64	0.13*	4×10^{-5}	−0.29	−0.01	0.8
S–P2	−0.37	−0.06	0.06	−0.96	−0.16*	2×10^{-7}
T–N1	0.64	0.10*	0.001	0.92	0.05	0.1
T–P2	0.56	0.12*	1×10^{-4}	−0.64	0.11*	5×10^{-4}
T–N2	−0.60	0.13*	6×10^{-5}	0.86	0.11*	7×10^{-4}
T–P3	−0.65	−0.04	0.2	0.51	−0.01	0.6
D_1	0.64	−0.05	0.1	−0.81	0.06*	0.04
D_2	−0.95	−0.07*	0.03	0.57	0.03	0.3

is generated by a different mechanism than the positivity with latency 100–150 ms clearly present in children under age 9. Hence, the positivity in young children is at best a superposition of adult P1 and P2 components, and thus neither its latency nor its amplitude can be meaningfully related to adult component scores.

There is also strong evidence to suggest that the positivity in young children includes a superimposed N1 component: as shown in Fig. 12, the difference in amplitudes between standard and target N1 remains virtually constant throughout development. This implies that an N1-like negativity is present even in very young children, as should be expected, since N1 appears to reflect attention to basic stimulus characteristics (Key et al., 2005), so the computational functions of which N1 is a correlate are presumably performed in young children. A plausible mechanism for the changes in the P1–N1–P2 complex that occur during development is the maturation of the upper cortical layers, whose pyramidal cells are inverted with respect to the neurons of lower layers

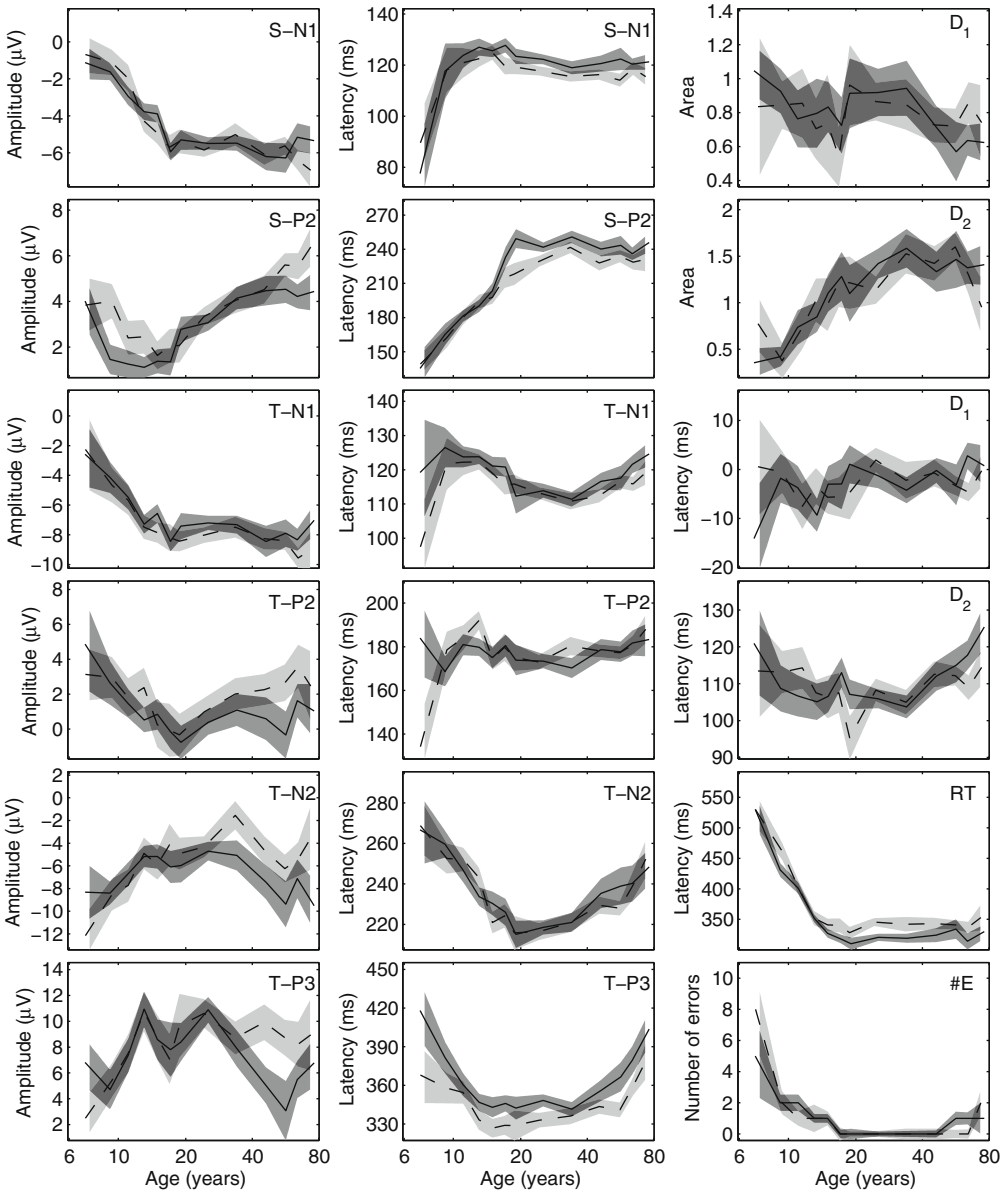

Fig. 11. Sex differences in component scores (S, standard; T, target), deconvolution peak quantifications (D_1, D_2), reaction time (RT), and error rate (#E) as a function of age (horizontal axes), calculated using a moving mean of 50 subjects. Plots show the mean and ±2 standard errors for males (solid line, dark shading) and females (dashed line, light shading). Age is plotted logarithmically to highlight the rapid changes during development.

Table 4
Comparison of latencies for male and female adult subjects (20–40 years) for standard N1, standard P2, target P3, and reaction time (RT). Mean values and standard errors are given.

Measure	Males (ms)	Females (ms)
S–N1	121 ± 1	117 ± 1
S–P2	240 ± 2	229 ± 2
T–P3	345 ± 3	335 ± 3
RT	329 ± 3	351 ± 4

(Eggermont and Ponton, 2003). This would produce a response of opposite polarity on the scalp, and hence change a net positivity to a net negativity.

The remainder of the waveform appears to be more easily interpreted. We propose that the negativity with latency ~250 ms in the standard and target waveforms of young children is an analog of target N2, since this component is continuous with adult N2 in targets. Additionally, it disappears from standards during age 10–12, which would be expected as the brain becomes more adept at suppressing unwanted stimuli. Strong support for this hypothesis comes from Čeponienė et al. (2002), who show that the scalp distribution of N2 does not change with age. Target P3 also appears to emerge during this age range, and is likely also related to improvements in determining task relevance. Only imprecise theories have been put forward to explain the increase in differentiation between standards and targets, usually relating to changes in synaptic density (Oades et al., 1997; Albrecht et al., 2000; Bishop et al., 2007). However, Čeponienė et al. (2002) found evidence, using dipole modeling, that new areas of the brain may become involved in the processing of stimuli during the course of development.

4.2. Component scores

A significant problem with traditional component scoring is that the morphologies of the AEP waveforms change dramatically during childhood and early adolescence. Since each component is usually defined as an extremum of a given sign within a given latency window, using adult definitions of components to score the waveforms of young children will yield either no results or incorrect ones. This is the most likely cause of the large variance in component latencies in young children, which declines sharply once the adult AEP morphology develops. Hence, all age trends in such component scores during development must be interpreted very cautiously, especially in relation to adult scores. However, the reductions in the latencies of target N2 and P3 appear to be robust results (Goodin et al., 1978; Barajas, 1990; Friedman and Simpson, 1994), and may be related to increasing myelination in the brain; this increases axonal transmission velocity and therefore speeds processing (Oades et al., 1997; Albrecht et al., 2000; Bishop et al., 2007).

Age trends in component scores in adults largely replicated the results of previous studies, although many more age trends were found to be statistically significant, due to the very large sample size used in this study. For each of the four component scores for which no significant age trends in adults were found (standard N1 amplitude, target N1 and N2 amplitudes, and target P2 latency), previous studies have reported conflicting results (Goodin et al., 1978; Pfefferbaum et al., 1980; Polich, 1997; Bahramali et al., 1999). In contrast to some previous studies (e.g., Goodin et al., 1978), the most statistically significant component score age trend we observed was an increase in standard P2 amplitude in adults, a trend which may result from decreased ability of the elderly to suppress unwanted stimuli (Amenedo and Díaz, 1998). The next two most statistically significant age trends we observed, increases in target N2 and P3 latency, have been consistently reported, although our estimates of the magnitudes of these trends (0.6 ms/year) are smaller than most previous results (e.g., Goodin et al., 1978; Brown et al., 1983). These latency changes are also well explained by changes in axonal myelination, since the amount of myelin (Sowell et al., 2004) and its quality (Peters, 2002) appear to decline after middle age. If latency changes were the result of a systemic reduction in transmission velocity, then this would imply a uniform fractional latency increase of AEP components. Despite the increases in the latencies of N2 and P3, no increase in reaction time was observed during aging, indicating that either (i) the motor response is not dependent upon the processing that occurs during these components, or (ii) the increased component latencies are compensated for by increased efficiency elsewhere in the motor pathway.

As shown in Fig. 13, there is a correlation between the latency of a component and the magnitude of its age trend, especially during development ($r^2 = 0.92$, excluding standard P2 latency as an

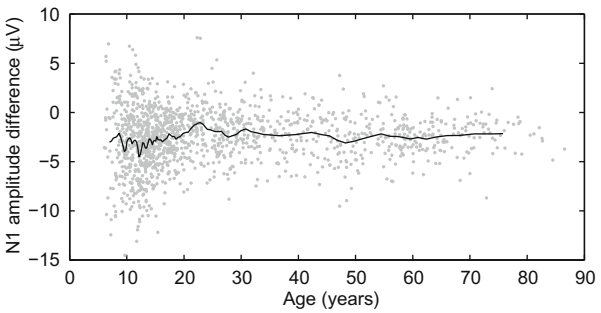

Fig. 12. Amplitude difference between target and standard N1 component scores, showing the difference for each subject (dots) and a moving average of 100 subjects across age (solid line). Despite considerable age-related changes in both standard and target N1 amplitudes, as shown in Fig. 6, the target-standard N1 amplitude difference is relatively constant across age.

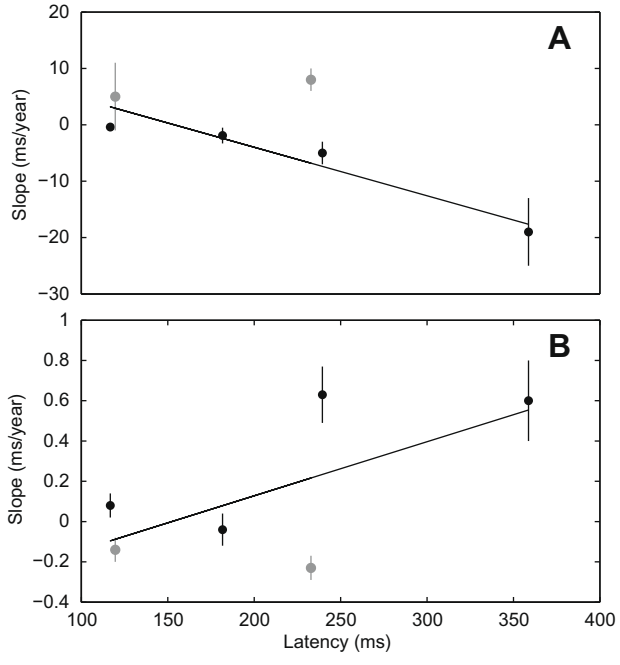

Fig. 13. Relationship between AEP component latencies and the rate at which these latencies change (i.e., the slope of their age trends) during (A) development and (B) aging. Each dot corresponds to a single component in standard (gray; N1 and P2) or target (black; N1, P2, N2, and P3) waveforms; vertical lines show ±2 standard errors. The lines of best fit are $y = -0.09x + 13$ for development and $y = 0.003x - 0.4$ for aging.

outlier). During aging, however, this relationship fairly is weak ($r^2 = 0.42$; cf. Goodin et al., 1978), and is instead more suggestive of two clusters: one comprised of target and standard N1 and P2 components, which show small or negligible aging trends in latency, and one comprised of target N2 and P3 components, which show considerable aging trends. Note that the average aging trends in each of these two clusters (-0.1 ± 0.1 and 0.6 ± 0.1 ms/year, respectively) match the aging trends in the deconvolution peak latencies (-0.07 ± 0.04 and 0.5 ± 0.1 ms/year, respectively). Since frontal white matter loss appears to be more dramatic than white matter loss in other areas of the brain (Sowell et al., 2004), this may explain why later components show larger fractional latency changes during aging. Additionally, since component amplitudes and latencies are interrelated, some of the inconsistencies in the latency age trends may be partly due to distortion by amplitude age trends.

If most EEG phenomena, including EPs, are the result of long-range cortical or corticothalamic interactions (Nunez, 1995; Robinson et al., 1997; Rennie et al., 2002), then we would predict that in addition to the decreases in AEP component latencies during development and increases during aging, there would be comparable changes in the latencies of visual and somatosensory EPs, as well as changes in the alpha peak frequency of the EEG spectrum. Tachibana et al. (1996) found increases in the latencies of late visual EP components of 1.2 ms/year during aging, and while this is larger than AEP latency trends reported here, it is consistent with the results of previous studies on AEP latencies (Brown et al., 1983; Bahramali et al., 1999). Taylor et al. (1999) found a change in visual N170 latency of approximately −10 ms/year in children aged 5–14, which is also somewhat more than would be expected from Fig. 13A. Somatosensory EP latencies are confounded by the effect of increasing axon lengths in the peripheral nervous system, but Allison et al. (1984) did find decreases in latency during development once this effect was taken into account. Alpha frequency appears to increase during development and decrease during aging (for review, see Klimesch, 1999), and this issue will be examined in detail in a forthcoming publication (Chiang et al., in preparation).

Strong correlations have previously been found between component scores (e.g., Fuchigami et al., 1993), and we have demonstrated that these correlations, when plotted against the mean latency difference of the components, have a well-defined upper bound that decreases with time. It is not known what the specific mechanism of these correlations are, why amplitudes show greater correlations than latencies, or why the correlations appear to show such a clear upper bound. However, systems of widely varying scale show behavior where correlations change over time (e.g., Kuramoto, 1984; Pfurtscheller and Lopes da Silva, 1999; Jarosiewicz et al., 2002), and future model-based work may provide further insight into this finding. In practice, the high degree of correlation between component scores limits their information content as a means of quantifying EPs, and provides further justification for the use of methods that remove this redundancy.

4.3. Deconvolution

Two distinct development-related changes occur in the AEP waveforms. First, some aspects of the waveforms undergo similar changes in both standards and targets, such as the "emergence" of N1. However, a second set of changes relates to improved differentiation between standards and targets, in that standard and target responses are very similar in young children, and become increasingly different with age. Although the deconvolution method used here does not provide any information on the first type of developmental change, it is the ideal tool for investigating the second. This change in task differentiation is difficult to quantify using component scoring, but deconvolution yields a striking result: at every age, the target response contains a standard, as shown by the presence at all ages of a peak in the deconvolution time series with a relative response latency of approximately zero and a relative response amplitude of approximately one. This implies that either (i) the cortical network(s) that generate standard responses are also always activated during target responses, or (ii) the network(s) that generate the first ~ 200 ms of the target response happen to be very similar to those that generate the same period of the standard response. Parsimony, and the similar topography of target and standard N1 components (Oades et al., 1995; Potts et al., 1998), favors the former interpretation.

During development (ages 6–12) a second peak emerges in the deconvolution time series, implying that in adults, the target response resembles two superimposed standard responses. This peak has a relative response latency of approximately 100 ms, and a relative response amplitude of approximately 1.5, and therefore corresponds to a delayed and amplified standard present in the target waveform. One possible physiological explanation for this result is that the target is produced by two thalamocortical (or corticocortical) impulses, causing the sequential activation of two anatomically and dynamically similar cortical networks. In this hypothesis, the time between the two impulses (~ 100 ms) is due to the thalamocortical loop delay (Rennie et al., 2002; Kerr et al., 2008), and the larger amplitude of the second impulse is due to an excitatory feedback loop.

A cognitive interpretation of the deconvolution peaks in adults can be based on the cognitive functions of the components in the original AEP waveforms. Since the first deconvolution peak loosely corresponds to N1 and P2 components, and the second peak to N2 and P3 components, we predict that the first peak would be largely "exogenous" (i.e., affected primarily by the physical characteristics of the stimuli; see Donchin et al., 1978), while the second would be largely "endogenous" (i.e., affected primarily by attention and task conditions). These predictions can be tested in future work by using stimuli with a range of physical and task characteristics. If these predictions are correct, the first deconvolution peak would correspond to basic stimulus processing, which would explain why it changes so little over the lifespan, while the second peak would reflect task-relevant aspects of stimulus processing.

These interpretations do not apply in young children, who show a single deconvolution peak. This result implies that standard and target stimuli are processed more similarly in children than they are in adults. Deconvolution alone cannot show whether the increasing difference between standards and targets is due to changes in the standard, changes in the target, or both. However, the age trends in waveform morphology described above (Section 4.1) indicate that this difference primarily arises from changes in the standard response. Cognitively, this result implies that all stimuli are treated as task-relevant by sufficiently young children, with the capacity for selective attention developing through late childhood and early adolescence.

In contrast to scoring, deconvolution uses the full lengths of the original AEP waveforms, and hence ideally the epoch length used would equal the interstimulus interval (ISI). In this study, AEP epochs extended from 0 to 600 ms relative to the stimulus (representing 60% of the ISI), which produced a deconvolution time series of 600 ms duration, chosen to be centered on zero (i.e., −300 to 300 ms relative to the standard waveform). Previously, deconvolution was applied to AEP data from −200 to 800 ms relative to the stimulus (100% of the ISI), which was used to produce a deconvolution time series extending from −200 to 800 ms (Kerr et al., 2009). Even with the shorter epoch length used here, deconvolution yielded meaningful peak areas and latencies. However, a greater epoch length would likely result in an improved signal-to-noise ratio, reduced artifact in the deconvolution time series, and decreased variances of peak areas and latencies.

4.4. Reaction time and error rate

Our data provide improved statistics supporting the findings of previous studies that reaction time decreases during development (e.g., Johnstone et al., 1996; Tachibana et al., 1996) but does not change during aging (e.g., Pfefferbaum et al., 1980; Fuchigami et al., 1993; Bahramali et al., 1999). The similarity of the age trends in reaction time and error rate, shown in Fig. 10, indicates that both speed and accuracy aspects of task performance mature with similar time courses, a result that is quantified by the strong positive correlation between their age trends ($\rho = 0.9$). The small negative correlation between reaction time and error rate residuals ($\rho = -0.1, p < 10^{-3}$) indicates that a subtle tradeoff between speed and accuracy does exist, and this correlation persists even when males and females or subjects above and below age 20 are analyzed separately.

In general, AEP measures were poorly correlated with reaction time in individual subjects, and none explained more than 3% of the total intersubject variance. Although the negative correlation between reaction time and standard P2 latency residuals cannot be due to chance ($\rho = -0.16, p < 10^{-6}$), this correlation may partially be the result of intersubject variability during development. For example, the disappearance of the ~ 250 ms negative component in children might be linked to improved stimulus discrimination (and hence to shorter reaction time), as well as to longer standard P2 latency (since the two components overlap), and hence variation in the age at which this occurs will lead to a correlation between residuals, even after age trends have been removed. The correlation between reaction time and standard P2 latency residuals does become much weaker when only subjects over 20 are analyzed, but it remains statistically significant unless all subjects under age 35 are excluded, indicating that it cannot be entirely explained by developmental effects.

The residuals of target P2 and N2 latencies show statistically significant positive correlations with reaction time residuals across all ages. These correlations are slightly stronger in subjects above 20 than those below 20, which is likely a result of the inherent difficulties of component scoring in children. The correlation between N2 latency and reaction time residuals ($\rho = 0.11, p < 10^{-3}$) is particularly interesting, since N2 is associated with stimulus discrimination (Key et al., 2005), a necessary prerequisite for reaction in the oddball paradigm. Although target N2 latency and reaction time age trends show a strong correlation ($\rho = 0.86$), the magnitudes of these age trends are very different during both development (-5 ± 1 and -50 ± 15 ms/year, respectively) and aging (0.6 ± 0.1 and 0.2 ± 0.2 ms/year, respectively), and hence N2 latency and reaction time do not appear to be directly linked.

There was a particularly strong correlation ($\rho = -0.95$) between age trends in reaction time and the area of the second peak in the deconvolution time series (D_2), suggesting that this measure may be a useful marker of the development of the networks required for fast and accurate reaction to a stimulus. The residuals of D_2 area and reaction time also showed a statistically significant correlation, but since this correlation vanishes when subjects under 20 are excluded, it appears to result from the same intersubject variability effect described above (i.e., children who mature early have larger D_2 area and shorter reaction times than other children of the same age).

4.5. Sex differences

No significant sex differences in age trends were found. Compared to males, females had shorter component latencies (yet longer reaction times) during adulthood, and more positive component amplitudes over some age ranges (typically about 40–60). These effects were generally small in comparison to age trends, however, and hence we found little need to control for the effects of sex. The finding of shorter latencies in females is well known, and is commonly explained in terms of brain size (Allison et al., 1983). While previous authors have speculated that females sacrifice speed for accuracy, thereby causing slower reaction times (Welford, 1988), we found no evidence of this (cf. Der and Deary, 2006). An alternative explanation is that much of the sex difference in reaction times is due to differences in peripheral aspects of the response, especially relative muscle mass (Nicholson and Kimura, 1996), and this may additionally explain why the sex difference in reaction times does not become significant until puberty.

4.6. Limitations and conclusions

Due to the large sample size used in this study, it was not possible to use a large variety of experimental conditions. For example, ISI and electrode position are known to have significant effects on the age trends observed in AEPs, but these could not be examined in the present study. It has been found that N1 can be elicited in children as young as three by using an ISI of several seconds or longer (Paetau et al., 1995; Čeponienė et al., 2002), in which case the differences in waveform morphology between children and adults are less pronounced. While frontal electrodes show similar age trends to Cz, parietal, occipital, and lateral electrodes often do not, especially for later components (Ponton et al., 2000). In general, age and scalp location both have such considerable effects on waveform morphology that scoring of the conventional components (P1, N1, P2, N2, P3) is often unfeasible (Ponton et al., 2002). In contrast, deconvolution may be an ideal method for the analysis of multichannel recordings, since scalp location tends to affect standard and target waveforms similarly.

An interesting extension of this study would be to examine age trends in children under age 6. Morphological changes in AEP waveforms are apparent from birth (Čeponienė et al., 2002), and can be related to stages of cortical development (Eggermont and Ponton, 2003). We predict that although AEP waveforms and component scores change considerably under age 6 (Wunderlich and Cone-Wesson, 2006), the deconvolution time series will not, since task differentiation (as indexed by AEP morphology) does not seem to appear until later in development.

In conclusion, this study is the largest analysis of AEP age trends to date. It provides quantifications of several previously unmeasured AEP properties (e.g., deconvolution peak areas and latencies, and the decrease in component score correlations over time), as well as improved statistics on a number of well-known age trends (e.g., P3 latency and reaction time). Additionally, these results demonstrate that deconvolution is a powerful method for examining age trends in AEPs, as it allows the development of task differentiation in children to be observed and quantified. Future work will analyze data from additional electrodes, investigate AEP and EEG age trends using physiology-based modeling (Kerr et al., 2008; Rowe et al., 2004), and relate these results to those of the present study.

Acknowledgements

We acknowledge the support of the Brain Resource International Database (under the auspices of Brain Resource; www.brainresource.com) for data acquisition and processing. All scientific decisions are made independently of any Brain Resource commercial decisions via the independently operated scientific division, BRAINnet (www.brainnet.net). We thank the individuals who gave their time to take part in the study. The Australian Research Council supported this work.

References

Albrecht R, von Suchodoletz W, Uwer R. The development of auditory evoked dipole source activity from childhood to adulthood. Clin Neurophysiol 2000;111:2268–76.

Allison T, Hume AL, Wood CC, Goff WR. Developmental and aging changes in somatosensory, auditory and visual evoked potentials. Electroencephalogr Clin Neurophysiol 1984;58:14–24.

Allison T, Wood CC, Goff WR. Brain stem auditory, pattern-reversal visual, and short-latency somatosensory evoked potentials: latencies in relation to age, sex, and brain and body size. Electroencephalogr Clin Neurophysiol 1983;55:619–36.

Amenedo E, Díaz F. Aging-related changes in processing of non-target and target stimuli during an auditory oddball task. Biol Psychol 1998;48:235–67.

Anderer P, Semlitsch HV, Saletu B. Multichannel auditory event-related brain potentials: effects of normal aging on the scalp distribution of N1, P2, N2 and P300 latencies and amplitudes. Electroencephalogr Clin Neurophysiol 1996;99:458–72.

Bahramali H, Gordon E, Lagopoulos J, Lim CL, Li W, Leslie J, et al. The effects of age on late components of the ERP and reaction time. Exp Aging Res 1999;25:69–80.

Barajas JJ. The effects of age on human P3 latency. Acta Otolaryngol Suppl 1990;476:157–60.

Bishop DV, Hardiman M, Uwer R, von Suchodoletz W. Maturation of the long-latency auditory ERP: step function changes at start and end of adolescence. Dev Sci 2007;10:565–75.

Brown WS, Marsh JT, LaRue A. Exponential electrophysiological aging: P3 latency. Electroencephalogr Clin Neurophysiol 1983;55:277–85.

Caviness VS, Kennedy DN, Richelme C, Rademacher J, Filipek PA. The human brain age 7–11 years: a volumetric analysis based on magnetic resonance images. Cereb Cortex 1996;6:726–36.

Čeponienė R, Rinne T, Näätänen R. Maturation of cortical sound processing as indexed by event-related potentials. Clin Neurophysiol 2002;113:870–82.

Der G, Deary IJ. Age and sex differences in reaction time in adulthood: results from the United Kingdom Health and Lifestyle Survey. Psychol Aging 2006;21:62–73.

Donchin E, Ritter W, McCallum WC. Cognitive psychophysiology: the endogenous components of the ERP. In: Callaway E, Tueting P, Koslow SH, editors. Event-related brain potentials in man. New York: Academic Press; 1978. p. 349–411.

Dujardin K, Derambure P, Bourriez JL, Jacquesson JM, Guieu JD. P300 component of the event-related potentials (ERP) during an attention task: effects of age, stimulus modality and event probability. Int J Psychophysiol 1993;14:255–67.

Dustman RE, Beck EC. The effects of maturation and aging on the wave form of visually evoked potentials. Electroencephalogr Clin Neurophysiol 1969;26:2–11.

Eggermont JJ, Ponton CW. Auditory-evoked potential studies of cortical maturation in normal hearing and implanted children: correlations with changes in structure and speech perception. Acta Otolaryngol 2003;123:249–52.

Friedman D, Simpson GV. ERP amplitude and scalp distribution to target and novel events: effects of temporal order in young, middle-aged and older adults. Brain Res Cogn Brain Res 1994;2:49–63.

Fuchigami T, Okubo O, Fujita Y, Okuni M, Noguchi Y, Yamada T. Auditory event-related potentials and reaction time in children: evaluation of cognitive development. Dev Med Child Neurol 1993;35:230–7.

Goodin DS, Squires KC, Henderson BH, Starr A. Age-related variations in evoked potentials to auditory stimuli in normal human subjects. Electroencephalogr Clin Neurophysiol 1978;44:447–58.

Gordon E, Cooper N, Rennie C, Hermens D, Williams LM. Integrative neuroscience: the role of a standardized database. Clin EEG Neurosci 2005;36:64–75.

Gratton G, Coles MGH, Donchin E. A new method for offline removal of ocular artifact. Electroencephalogr Clin Neurophysiol 1983;55:468–84.

Haig AR, Gordon E, Rogers G, Anderson J. Classification of single-trial ERP sub-types: application of globally optimal vector quantization using simulated annealing. Electroencephalogr Clin Neurophysiol 1995;94:288–97.

Hansen JC. Separation of overlapping waveforms having known temporal distributions. J Neurosci Methods 1983;9:127–39.

Jarosiewicz B, McNaughton BL, Skaggs WE. Hippocampal population activity during the small-amplitude irregular activity state in the rat. J Neurosci 2002;22:1373–84.

Jewett DL, Caplovitz G, Baird B, Trumpis M, Olson MP, Larson-Prior LJ. The use of QSD (q-sequence deconvolution) to recover superposed, transient evoked-responses. Clin Neurophysiol 2004;115:2754–75.

Johnstone SJ, Barry RJ, Anderson JW, Coyle SF. Age-related changes in child and adolescent event-related potential component morphology, amplitude and latency to standard and target stimuli in an auditory oddball task. Int J Psychophysiol 1996;24:223–38.

Kerr CC, Rennie CJ, Robinson PA. Physiology-based modeling of cortical auditory evoked potentials. Biol Cybern 2008;98:171–84.

Kerr CC, Rennie CJ, Robinson PA. Deconvolution analysis of target evoked potentials. J Neurosci Methods 2009;179:101–10.

Key AP, Dove GO, Maguire MJ. Linking brainwaves to the brain: an ERP primer. Dev Neuropsychol 2005;27:183–215.

Klimesch W. EEG alpha and theta oscillations reflect cognitive and memory performance: a review and analysis. Brain Res Rev 1999;29:169–95.

Kraiuhin C, Gordon E, Coyle S, Sara G, Rennie C, Howson A, et al. Normal latency of the P300 event-related potential in mild-to-moderate Alzheimer's disease and depression. Biol Psychiatry 1990;28:372–86.

Kuramoto Y. Chemical oscillations, waves, and turbulence. Berlin: Springer; 1984.

Martin L, Barajas JJ, Fernandez R, Torres E. Auditory event-related potentials in well-characterized groups of children. Electroencephalogr Clin Neurophysiol 1988;71:375–81.

Miller A, Alston R, Corsellis J. Variation with age in the volumes of grey and white matter in the cerebral hemispheres of man—measurements with an image analyzer. Neuropath Appl Neurobiol 1980;6:119–32.

Nelder JA, Mead R. A simplex method for function minimization. Comput J 1965;7:308–13.

Nicholson KG, Kimura D. Sex differences for speech and manual skill. Percept Mot Skills 1996;82:3–13.

Nunez PL. Neocortical dynamics and human EEG rhythms. New York: Oxford University Press; 1995.

Oades RD, Dittmann-Balcar A, Zerbin D. Development and topography of auditory event-related potentials (ERPs): mismatch and processing negativity in individuals 8–22 years of age. Psychophysiology 1997;34:677–93.

Oades RD, Zerbin D, Dittmann-Balcar A. The topography of event-related potentials in passive and active conditions of a 3-tone auditory oddball test. Int J Neurosci 1995;81:249–64.

Özdamar Ö, Bohórquez J. Signal-to-noise ratio and frequency analysis of continuous loop averaging deconvolution (CLAD) of overlapping evoked potentials. J Acoust Soc Am 2006;119:429–38.

Paetau R, Ahonen A, Salonen O, Sams M. Auditory evoked magnetic fields to tones and pseudowords in healthy children and adults. J Clin Neurophysiol 1995;12:177–85.

Peters A. Structural changes that occur during normal aging of primate cerebral hemispheres. Neurosci Biobehav Revl 2002;26:733–41.

Pfefferbaum A, Ford JM, Roth WT, Kopell BS. Age-related changes in auditory event-related potentials. Electroencephalogr Clin Neurophysiol 1980;49:266–76.

Pfurtscheller G, Lopes da Silva FH. Event-related EEG/MEG synchronization and desynchronization: basic principles. Clin Neurophysiol 1999;110:1842–57.

Piguet O, Double KL, Kril JJ, Harasty J, Macdonald V, McRitchie DA, et al. White matter loss in healthy ageing: a postmortem analysis. Neurobiol Aging 2009;30:1288–95.

Polich J. EEG and ERP assessment of normal aging. Electroencephalogr Clin Neurophysiol 1997;104:244–56.

Ponton C, Eggermont JJ, Khosla D, Kwong B, Don M. Maturation of human central auditory system activity: separating auditory evoked potentials by dipole source modeling. Clin Neurophysiol 2002;113:407–20.

Ponton C, Eggermont JJ, Kwong B, Don M. Maturation of human central auditory system activity: evidence from multi-channel evoked potentials. Clin Neurophysiol 2000;111:220–36.

Potts GF, Hirayasu Y, O'Donnell BF, Shenton EM, McCarley RW. High-density recording and topographic analysis of the auditory oddball event-related potential in patients with schizophrenia. Biol Psychiatry 1998;44:982–9.

Rennie CJ, Robinson PA, Wright JJ. Unified neurophysical model of EEG spectra and evoked potentials. Biol Cybern 2002;86:457–71.

Robinson PA, Rennie CJ, Wright JJ. Propagation and stability of waves of electrical activity in the cerebral cortex. Phys Rev E 1997;56:826–40.

Rowe DL, Robinson PA, Rennie CJ. Estimation of neurophysiological parameters from the waking EEG using a biophysical model of brain dynamics. J Theor Biol 2004;231:413–33.

Segalowitz SJ, Barnes KL. The reliability of ERP components in the auditory oddball paradigm. Psychophysiol 1993;30:451–9.

Sowell ER, Thompson PM, Toga AW. Mapping changes in the human cortex throughout the span of life. Neuroscientist 2004;10:372–92.

Tachibana H, Aragane K, Sugita M. Age-related changes in event-related potentials in visual discrimination tasks. Electroencephalogr Clin Neurophysiol 1996;100:299–309.

Taylor MJ, McCarthy G, Saliba E, Degiovanni E. ERP evidence of developmental changes in processing of faces. Clin Neurophysiol 1999;110:910–5.

Ungan P, Başar E. Comparison of Wiener filtering and selective averaging of evoked potentials. Electroencephalogr Clin Neurophysiol 1976;40:516–20.

van Albada SJ, Rennie CJ, Robinson PA. Variability of model-free and model-based quantitative measures of EEG. J Integ Neurosci 2007;6:279–307.

Wang T, Özdamar Ö, Bohórquez J, Shen Q, Cheour M. Wiener filter deconvolution of overlapping evoked potentials. J Neurosci Methods 2006;15:260–70.

Wastell DG. When Wiener filtering is less than optimal: a illustrative application to the brain stem evoked potential. Electroencephalogr Clin Neurophysiol 1981;51:678–82.

Welford AT. Reaction time, speed of performance, and age. Ann N Y Acad Sci 1988;515:1–17.

Wiener N. Extrapolation, interpolation and smoothing of stationary time series with engineering applications. Cambridge, MA: M.I.T. Press; 1949.

Williams LM, Gatt JM, Hatch A, Palmer DM, Nagy M, Rennie C, et al. The Integrate model of emotion, thinking, and self regulation: an application to the "Paradox of Aging". J Int Neurosci 2008;7:367–404.

Woldorff MG. Distortion of ERP averages due to overlap from temporally adjacent ERPs: analysis and correction. Psychophysiology 1993;30:98–119.

Wright JJ, Sergejew AA, Stampfer HG. Inverse filter computation of the neural impulse giving rise to the auditory evoked potential. Brain Topogr 1990;2:293–302.

Wunderlich JL, Cone-Wesson BK. Maturation of CAEP in infants and children: a review. Hear Res 2006;212:212–23.